Resilient Cities and Structures 2 (2023) 91–102

Contents lists available at ScienceDirect

Resilient Cities and Structures

journal homepage: www.elsevier.com/locate/rcns

Full Length Article

Numerical studies on the seismic response of a three-storey low-damage steel framed structure incorporating seismic friction connections

Zhenduo Yan[a], Shahab Ramhormozian[b,*], G. Charles Clifton[a], Rui Zhang[c], Ping Xiang[d], Liang-Jiu Jia[c,f,*], Gregory A. MacRae[e], Xianzhong Zhao[d,f]

[a] Department of Civil and Environmental Engineering, The University of Auckland, Auckland, New Zealand
[b] Department of Built Environment Engineering, Auckland University of Technology, Auckland, New Zealand
[c] Department of Disaster Mitigation for Structures, Tongji University, Shanghai, China
[d] Department of Structural Engineering, Tongji University, Shanghai, China
[e] Department of Civil and Natural Resources Engineering, University of Canterbury, Christchurch, New Zealand
[f] State Key Laboratory of Disaster Reduction in Civil Engineering, Tongji University, Shanghai, China

ARTICLE INFO

Keywords:
Friction-based connection
Low damage
ILEE
ROBUST

ABSTRACT

A 9 m high, near full scale three-storey configurable steel frame composite floor building incorporating friction-based connections is to be tested using two linked bi-directional shake tables at the International joint research Laboratory of Earthquake Engineering (ILEE) facilities, Shanghai, China, as part of the RObust BUilding SysTem (ROBUST) project. A total of nine structural configurations are designed and detailed. To have a better understanding of the expected system behaviour, as well as effects of other structural and non-structural elements (NSEs) on the overall system response, experimental testing at component level has been conducted prior to the shake table testing. This paper presents an introduction to the ROBUST project, followed by a numerical study on one of the nine configurations of the structure, having Moment Resisting Steel Frame (MRSF) in the longitudinal direction and Concentrically Braced Frame (CBF) in the transverse direction. Hysteretic properties employed in the numerical models are validated against component test results. The predictions of the building's seismic response under selected base excitations are presented indicating the likely low damage performance of the structure.

1. Introduction

Many structures satisfied the life-safety condition during the severe 2010/2011 Canterbury earthquakes but were damaged to the extent that the structures were considered unsuitable for continued operation, requiring them to be demolished [1]. This has imposed significant economic pressure and business interruptions on the city and country. Efforts have been made to produce structures which have minor or no damage in major earthquake events so that they remain accessible and functional [2–5]. Some of these use base isolations and/or different types of energy dissipation mechanisms. One of the technologies which limits structural damage is to incorporate low-damage friction connections in moment resisting or braced frame systems. These friction connections are cost-effective and can limit the possibility and degree of damage to the main structural members. This research seeks to demonstrate the performance of such systems through the RObust BUilding SysTem (ROBUST) project [6–10]. This is a collaborative New Zealand - China project, involving the shaking table testing of a full scale multistorey resilient and repairable structural steel building system, with a representative floor diaphragm, friction connections and the full range of non-structural elements (NSEs), subject to 2D horizontal shaking. The testing will be conducted at the International Joint Research Laboratory on Earthquake Engineering (ILEE) facilities, Shanghai, China. This paper presents a numerical study on one of the nine configurations of the proposed structure incorporating friction connections at beam-to-column and brace-to-gusset plate locations, the properties of which were validated against experimental results from component tests reported as per [11]. The purpose of this study is to predict the seismic response of the building under selected base excitations.

2. ROBUST test program and building configuration

The proposed structure designed and detailed for this research is intended to emulate a typical building, such as an office building. The building systems are representative of a realistic building, and the primary energy dissipation mechanism will be provided by a range of frictional systems, many of which have been developed in New Zealand [12–18]. The structure is a 3-storey steel frame building with plan

* Corresponding authors.
E-mail addresses: shahab.ramhormozian@aut.ac.nz (S. Ramhormozian), lj_jia@tongji.edu.cn (L.-J. Jia).

https://doi.org/10.1016/j.rcns.2023.02.007
Received 18 December 2022; Received in revised form 2 February 2023; Accepted 12 February 2023

Table 1
Seismic weight of the structure at different levels.

Level	Height (m)	Seismic weight (kN)
3	9	276
2	6	251
1	3	251
Total	N/A	779

dimensions of 7250 mm by 4750 mm (from centre to centre) and an inter-storey height of 3 m, as shown below:

The building is considered to be of normal importance, i.e. Importance Level 2 as per NZS 1170.0 [19], and is located on shallow soil, i.e., Subsoil Class C as per NZS 1170.5 [20], in the Wellington CBD, within 8 km of the nearest fault. The composite flooring system with trapezoidal steel deck and concrete topping is used, which is also considered as the permanent load on the structure. The slab depth is 150 mm while the effective (i.e., average) thickness for mass calculation is 121 mm. To simulate the imposed load, additional mass blocks are to be used for different stories. The summation of the permanent loads (concrete floors and members) and the imposed loads (additional mass blocks) forms the seismic weight of the structure (see Table 1).

The structural systems considered for the whole ROBUST test program are shown in Table 2. There are four main types of structural systems considered, namely: Moment Resisting Steel Frame (MRSF), Concentrically Braced Frame (CBF), Rocking Steel Braced Frame (RSBF) incorporating a tension only GripNGrab (GNG) device [13] in the transverse direction, and beam-through Multiple Rocking Column (MRC) [14]. There are three different types of MRSF. The first type is using Sliding Hinge Joint (SHJ) with Asymmetric Friction Connection (AFC) [15] as the beam to column connections in one bay with another bay pinned, named MRF-SHJ. The second type is using resilient slip friction joint (RSFJ) [16] in one bay with another bay pinned at the beam to column connections (noted as MRF-RSFJ). The third type is using Optimised SHJs (OSHJs) [17] in one bay, with another bay pinned at the beam to column connection, named MRF-OSHJ. There are four types of CBF considered, namely: 1) CBF with single diagonal brace effective in compression and tension using a Symmetric Friction Connection (SFC) with Belleville Springs (SFCBeSs) connecting brace to the gusset plate, 2) CBF with single diagonal brace effective in compression and tension using RSFJ, 3) CBF with brace effective in tension only (TOB) using RSFJ [18], and 4) V-braced CBF with braces effective in compression and tension (CTB) using SFCBeSs at brace to gusset plate connection.

The structural system is designed and detailed to configure the changes from one seismic resisting system to another, while the gravity system remains stable on the shaking table. This has required careful consideration of connection design and detailing and overall structural stability and will be achieved by removing connection components associated with one type of seismic resisting and replacing them with those for the new system, while keeping the gravity system intact and stable

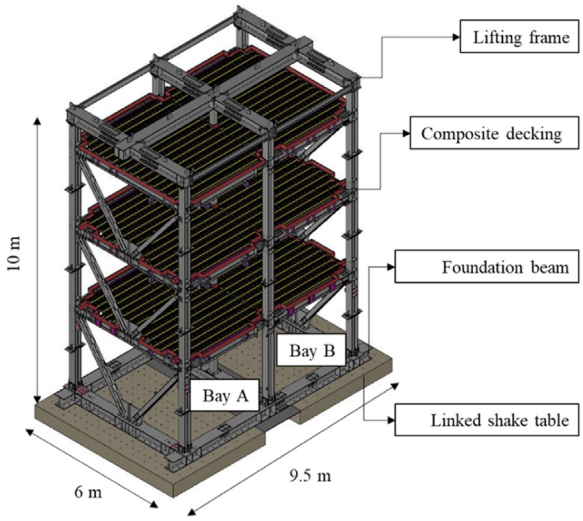

Fig. 1. Isometric view of the structure on linked shake table with lifting frame on top.

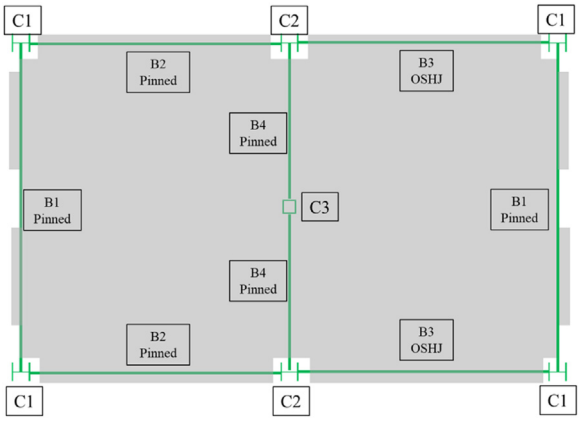

Fig. 2. Plan view of the structure.
Note: the extent of the concrete in the floor system is shown in grey.

NSEs [10] will be installed on the structure after the testing of first three major types. The structure will then be tested with full NSEs (type 4 in Table 2).

This paper is focused on the structural systems having the MRSF incorporating OSHJ in the longitudinal (long) direction and the V-braced CBF with brace effective in compression and tension using SFCBeSs in the transverse (short) direction (see Fig. 1), i.e. Type 2-subtype c. The

Table 2
Considered structural systems.

Type	Subtype	Longitudinal (X)		Transverse (Y)
		Bay A	Bay B	
1	a	CBF CTB RSFJ	Pinned*	CBF SFC
	b	CBF TOB RSFJ	Pinned	CBF SFC
	c	MRF-RSFJ	Pinned	CBF-SFCBeSs
2	a	Pinned	CBF-SFCBeSs	CBF-SFCBeSs
	b	Pinned	MRF-SHJ	CBF-SFCBeSs
	c	Pinned	MRF-OSHJ	CBF-SFCBeSs
3	a	Pinned	MRF-SHJ	RSBF
	b	Pinned/ MRF-RSFJ	MRF-OSHJ/ Pinned	MRC
4	(with NSE)	Pinned	MRF-OSHJ	CBF SFCBeSs

* Pinned refers to the beam to column connection.

Table 3
Frame section properties.

Member	Code	Section*	Cross-sectional area (mm^2)	Moment of inertia in major axis (mm^4)
Column	C1	250UC89.5	11,400	143×10^6
	C2	250UC89.5	11,400	143×10^6
	C3	200 × 200 × 10 SHS	7600	45.9×10^6
Beam	B1	310UB40.4	5210	86.4×10^6
	B2	310UB40.4	5210	86.4×10^6
	B3	310UB40.4	5210	86.4×10^6
	B4	310UB40.4	5210	86.4×10^6
Brace	BRC	160 × 80 × 6 RHS (back-to-back)	5472	17.9×10^6

Terminology for Table: UC – univerisal column; UB – universial beam; SHS – square holow section; RHS – rectangle holow section.

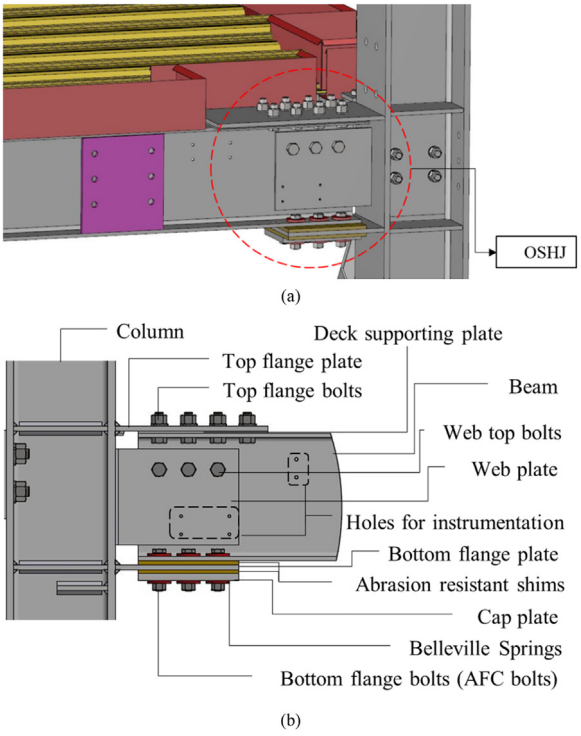

Fig. 3. OSHJ detail: (a) overview and (b) layout.

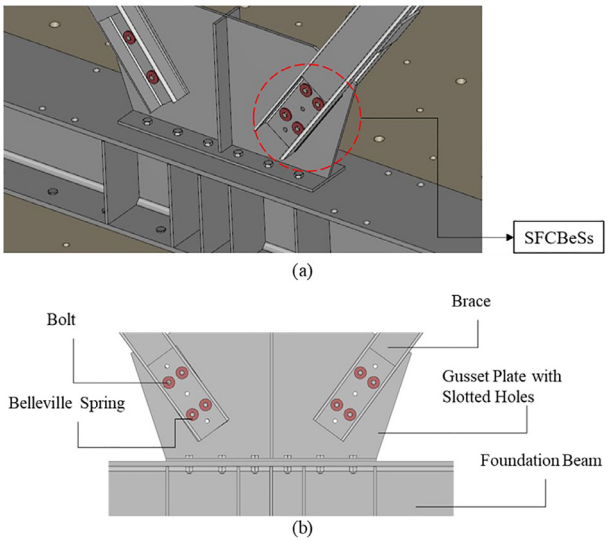

Fig. 4. Brace to gusset plate connection using SFCBeSs: (a) overview and (b) layout.

plan view of the structure is given in Fig. 2. The sections of the beam, brace and column are listed in Table 3.

The SHJ was developed by Charles Clifton [15] between 1998 and 2005 as a semi-rigid joint for low-damage seismic resisting system, primarily for MRSF. The OSHJ (see Fig. 3) is an optimised version of SHJ with the use of partially squashed Belleville Springs with bolts installed in elastic range [21–23], retaining installed bolt tension following severe events. The beam top flange is bolted into the top flange plate extending from the column flange, which establishes the point of rotation. The shear force in the beam is designed to be carried by the top web bolts. Horizontally slotted holes are provided in the bottom flange plate to allow significant rotations of the beam end relative to the column face. A "beam clearance" away from the column face is provided to accommodate the rotation demands under severe earthquake events. The bottom most plate in this assembly is the bottom flange cap plate, with no physical connection to the rest of the joint apart from through the bolts. High hardness abrasion resistant shims are used where sliding is designed to occur. The sliding shear force from the AFC bolts at beam bottom flange level becomes the fuse of the joint, which suppresses the yielding of other secondary elements within the design level.

Extending the concept of using Belleville Springs in an AFC, the SFCBeSs is designed and detailed as an optimised version of the sliding friction connection [22]. The connection can provide an efficient means of seismic energy dissipation, protecting the braces, collector beams and columns with comparable cost. The brace to midspan gusset plate connection is designed using SFCBeSs with long slotted holes, while the other side is designed with normal size hole. 4 Grade 8.8 M12 High Strength Friction Grip (HSFG) bolts are used, each with a pair of Belleville Springs one under the bolt head and one under the nut (see Fig. 4). The endplate of the midspan gusset plate is bolted into the foundation beam (or collector beam for upper levels).

As for the column base connection, a column strong axis aligned Asymmetric Friction Connection (SAFC Base [24]) is designed and detailed at external columns, as shown in Fig. 5. It can be considered as a 90-degree rotated SHJ. The AFC bolts are designed to slide under the ultimate limit state design level earthquake. The SAFC base can be configured to represent a nominal fixed or nominal pinned base condition, by adjusting the level of AFC bolts clamping force. With a much higher clamping force, there will be no sliding of the AFC bolts, the column base connection can be considered as nominally fixed. In contrast, with a much lower clamping force, there will be negligible resistance from AFC bolts, the column base connection can be considered as nominally pinned. The vertical plate connection to the web is used when uplift should be suppressed beyond specified limits.

The centre column (C3) is designed and detailed to carry gravity load only and to accommodate imposed seismic drift deformations through web side plate connections that are detailed to accommodate at least 30 milliradians of plastic rotation between the beam and column without loss of vertical load carrying capacity or horizontal attachment between beam and column [25,26]. The corner columns (C1) are subjected to

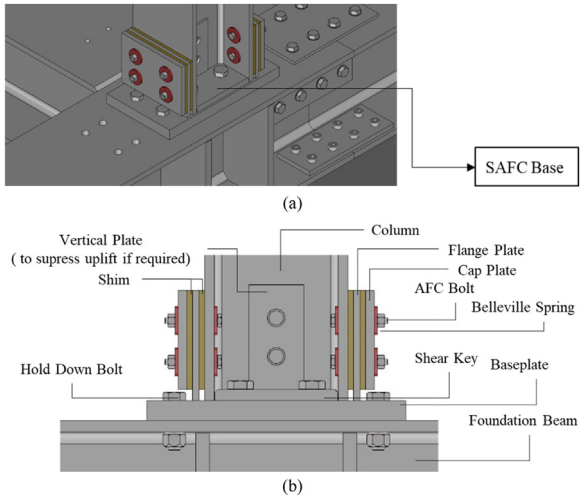

Fig. 5. SAFC Base (a) overview and (b) layout.

seismic actions from two different orthogonal seismic resisting systems (i.e. MRF-OSHJ in the longitudinal direction and CBF-SFCBeSs in the transverse direction) during bi-directional shaking and therefore are designed for concurrent actions. The collector beams (B1) and longitudinal beams (B2 and B3), unlike current practice, are not fully covered by the floor slab around the column corners (as shown in Fig. 2). Such gap allows the connections to be exposed and accessible, to assist with changeover activities between different structural systems on the main building.

3. MRF-OSHJ configuration

A MRSF is defined as: "a structural system of rigid or semi-rigid construction capable of resisting design loads or effects principally through the bending resistance of its members and connections" as per NZS3404 [27]. In the MRF-OSHJ configuration, the OSHJ is designed and detailed at beam to column connection in the longitudinal direction of the structure. The MRF-OSHJ is designed to remain elastic under serviceability limit states (SLS). When the imposed demand exceeds the ultimate limit state (ULS) design moment capacity, sliding commences at the OSHJ, allowing column rotation relative to the beam, dissipating energy and limiting internal actions in the beams and columns. At the end of the earthquake events, the OSHJ seizes up and become effectively rigid again. Comparing with a rigid MRSF, the use of OSHJ allows the elastic strength and stiffness to be decoupled and the primary mechanism is no longer material yielding. The OSHJ design moment can be set equal to the derived design earthquake moment as per NZS1170.5 [20], independent of the beam section moment capacity. The design actions on the column stiffeners, panel zones, column size and foundation can thus be reduced accordingly. The focus of this section is to show the design procedures and develop a representative numerical model of the MRF-OSHJ to be tested on the shake table.

3.1. Member design using ESM to NZS1170.5

The preliminary design procedure for the MRF-OSHJ concept follows a similar procedure for that of category 2 MRSF with rigid beam to column connections as per cl. 12.10 NZS3404 [27] and HERA R4–156 [28]. The OSHJ becomes the primary members, the columns and beams become the secondary members. The beams are designed to resist the overstrength capacity of the OSHJ plus vertical loading associated with earthquake without becoming inelastic. They are also designed to carry the full factored vertical loading simply supported. Design of columns for the load combinations including earthquake follows the capacity design procedure, through designing them to take the lesser of the following actions:

1) The capacity design derived design actions from the MRSF responding as a plastic mechanism with every connection developing its overstrength action and taking the upper limit action assuming ductility factor, $\mu = 1.25$;
2) The upper limit earthquake actions determined using the structural ductility factor, $\mu = 1.25$ in conjunction with the associated vertical actions.

Table 4
Modal periods for the MRF-OSHJ concept.

Mode number	Mode period (s)
1	1.15
2	0.25
3	0.12

Table 5
SLS and ULS base shears from ESM for the MRF-OSHJ concept.

Limit state	Return period factor R	μ	S_p	Base shear (kN)
SLS	0.25	1	0.7	59.7
ULS	1	3	0.7	79.6
EQmax	1	1.25	0.7	191.1

Following the preliminary design procedure, a 3D numerical model is then set up in SAP 2000 [29] with rigid diaphragm based on the geometry of the proposed structure on shake table. The floor load is assigned to beams according to the tributary area directly, considering slabs are isolated from columns to assist with changeover activities. Rigid diaphragm is assigned. NSEs are not considered. The rotational stiffness at external column bases (C1 and C2 as shown in Fig. 2) are assigned to be nominally pinned as per cl.4.8.3.4.1 NZS3404 [27]. Elastic rotational link is used at the beam-to-column connection, initially set as fully rigid, in one bay (circled in red, see Fig. 6(a)) while the beam-to-column connection at the other bay is set as pinned. The elevation view of the model in SAP 2000 is shown in Fig. 6(b), representing the MRF-OSHJ in the longitudinal direction. The beams in left hand side bay are not physically connected to the columns to show moment release (rotational stiffness is taken as zero) in Fig. 6(b). Once the initial demand of the OSHJ, which are based on ESM actions, is determined, the elastic rotational stiffness, k_e, should be applied, estimated as per Eq. (1) [15]:

$$k_e = \min\left(\frac{EA_{bfp}}{L} \times d_b^2,\ \frac{M_{OSHJ} \times 10^3}{\theta_{min}}\right) \quad (1)$$

where

L = distance from column face to the centre of first AFC bolt group
d_b = depth of incoming beam
A_{bfp} = area of bottom flange plate
E = 205 GPa
M_{OSHJ} = design sliding moment capacity of the OSHJ [15,21]
θ_{min} = 1.5 milliradians (mrads), practical lower value avoiding unrealistically high stiffness [15]

Iterations may be required to finalize the hysteretic property for the OSHJ, to match the derived design earthquake moment. A modal analysis is then performed. The obtained modal periods are given in Table 4.

The first two modes are the translational modes and the third mode is a torsional mode. The design base shear under SLS, ULS as well as upper limit base shear (noted as EQmax) are given Table 5.

It is worth noting that the structural performance factor, S_p, is taken as 0.7 as per NZS1170.5 [20] although there will be no NSEs, unlike a real building, on the structure at the time of testing for Type 2.c. The S_p factor is kept constant during the scaling of the earthquake

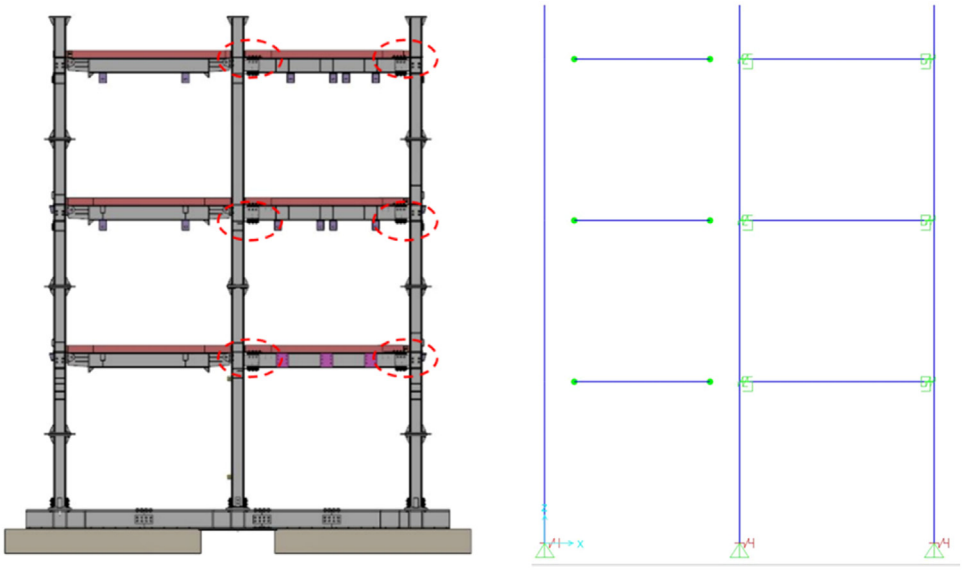

Fig. 6. MRF-OSHJ in the longitudinal direction (a) structural drawing and (b) layout of numerical model.

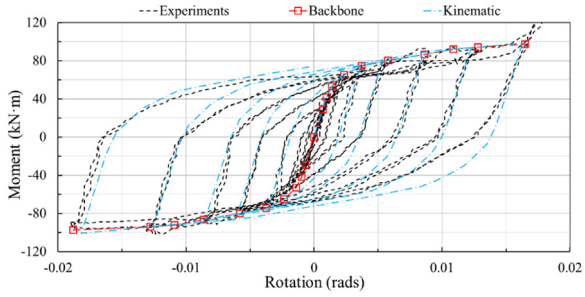

Fig. 7. Comparison of results for OSHJ beam-to-column subassembly.

records for time history analyses. Following this initial design, nonlinear pushover and time-history analyses have been carried out to study the performance of the MRF-OSHJ concept more accurately and also to check the adequacy of the OSHJ design. For this purpose, the nonlinear behaviour of the OSHJ should be defined in SAP2000 [29] using nonlinear rotational links. Instead of assuming an elastic perfect plastic behaviour [30], experimental testing at real scale component level [11] was designed and conducted to capture the full hysteretic property in the post-elastic range. The Multilinear plastic kinematic hysteretic model [29] was then found to be suitable to generate the OSHJ hysteresis curve, based on the backbone curve of the experimental results. A comparison of experimental and simulated results is given in Fig. 7. The strength deterioration if the sliding reaches the end of the slotted holes has not been considered in this model, however, a check has been made on the maximum rotational demand which shows that the end of the slotted holes will not be reached. The original development of the SHJ with AFCs [15] and the OSHJ [23] has determined the effects of the connection reaching the end of the slotted holes and quantified this on the component and system response.

3.2. Nonlinear static pushover analysis

A pushover analysis has been carried out in SAP2000 [29] to examine the yield displacements of the MRF-OSHJ (when sliding commences at the OSHJ) and succeeding inelastic behaviour. The lateral load pattern applied follows NZS1170.5 [20] which takes some allowance of higher mode effect into consideration through the application of 8% of the base shear at the top level of the seismic resisting system. The magnitude of the lateral loads is incrementally increased until the top of the central gravity column (C3) reaches the target displacement. As the purpose of this test is to have no structural damage up to Maximum Considered Events (MCE), the OSHJ is are designed to accommodate MCE rotation demand by providing sufficient slotted length. The ULS drift limit for designing the OSHJ is $2.5\%/k_{dm}$, where the drift modification factor, k_{dm}, is taken as 1.2 as per clause 7.3.1.1 of NZS1170.5 [20]. However, recommendations are given to control the inter-storey drift within 1.5% to reduce the extent of shaking-related damage on facades, fit-out and services by Gledhill et al. [31]. Hence, the target ULS drift is set to be 1.5%. The MCE level is taken as 1.8 times of the ULS drift [20]. As a result, the target displacement at the top of the structure for ULS and MCE levels is 135 and 243 mm, respectively.

Fig. 8(a) shows the pushover response of the structure where the bi-linear curve is also shown in red dashed line. Before reaching the SLS base shear from ESM, the corresponding displacement is less than the SLS displacement limit used in New Zealand practice [19] which is 0.33% or 29.7 mm for the proposed structure, indicating that there is no slippage of the OSHJ. The OSHJ commences to slide after the base shear exceeds the ULS design base shear from the ESM. Reverse sliding can be observed through a second pushover load cases from the end of previous pushover load case, pushing the structure from the target displacement in the positive direction to the target displacement in the negative direction and a third pushover load case, pushing the structure back to the original position, to illustrate a full cycle response of the MRF-OSHJ, as shown in Fig. 8(b).

3.3. Nonlinear Time History Analysis (NLTHA)

3.3.1. Selection of earthquake records

The direct-integration nonlinear time-history analysis was conducted in SAP2000 [29] using three records developed by Oyarzo-Vera et al. [32] for the North Island of New Zealand. The details of the selected records as well as the product of the record scale factor, k_1, and the family record factor, k_2, scaled to ULS are given in Table 6. k_1 adjusts a single record to match the design spectrum over the period range of interest while k_2 ensures the envelop of a family of records sits above the target spectrum over the period of interest.

Table 6
Selected ground motions characteristics.

No.	Record name	Date	Magnitude*	Fault mechanism	$k_1 \times k_2$
1	EI Centro, USA	19/05/1940	7.0	Strike slip	1.34 (2.41)
2	La Union, Mexico	19/09/1985	8.1	Subduction interface	2.26 (4.10)
3	Tabas, Iran	16/09/1978	7.4	Reverse	1.81 (3.26)

* The magnitude is in moment magnitude scale.

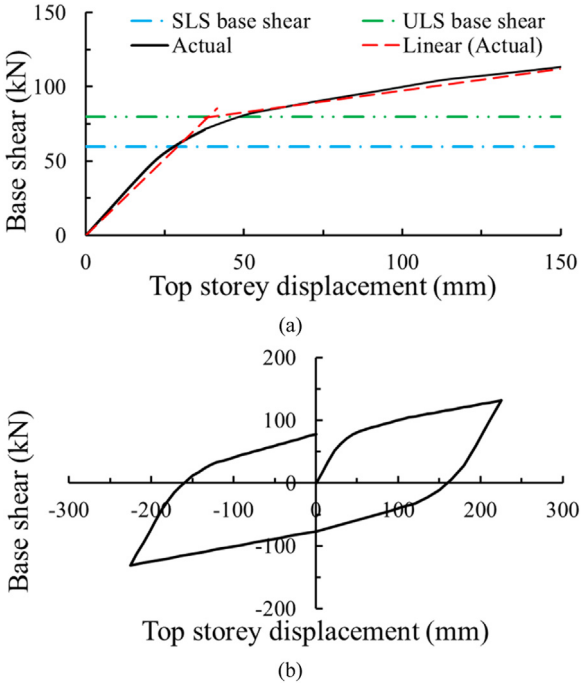

Fig. 8. Nonlinear static responses of the MRF-OSHJ concept: (a) uniaxial pushover and (b) full quasi-static response.

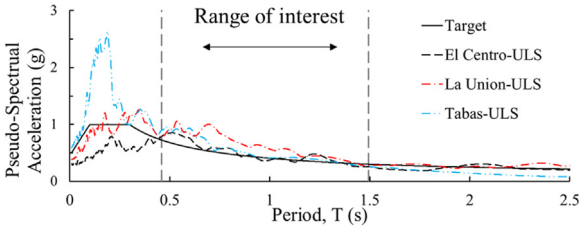

Fig. 9. Target and scaled records pseudo acceleration spectra.

The period of interest covers $0.4T_1$ to $1.3T_1$, where T_1 is the largest translational period in the direction being considered. The upper limit is intended to allow some lengthening of the period during inelastic response and the lower limit is to include some higher-mode response [20].

The spectra (see Fig. 9) are scaled to match the design basis earthquake, which refers to an earthquake with a 500-year return period that stands for the earthquake having 10% probability of exceedance in 50 years. In order to obtain the Maximum Considered Earthquake (MCE) scaled records with 2500-year return period, standing for the earthquake having 2% probability of exceedance in 50 years, a factor of 1.8 is required to be multiplied by the ULS scaled factor as per NZS1170.5 [20].

3.3.2. *Dynamic responses of MRF-OSHJ*

The base shear response of the structure is shown in Fig. 10 under MCE events. The maximum base shear in the positive direction is reached under the Tabas event and the maximum base shear in the negative direction is reached under La Union event. The hysteretic response of the OSHJ at critical level (level 1 – exhibiting highest demand) is shown in Fig. 11 and is within 30 mrads rotation under considered MCE events. The maximum positive rotation is reached under La Union event and the maximum negative direction is reached under El Centro event.

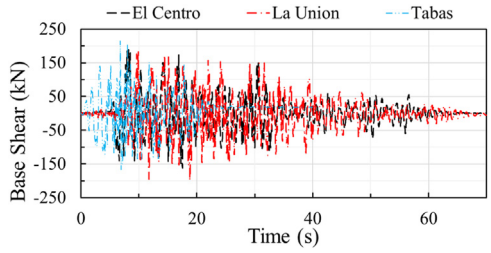

Fig. 10. Base shear responses of the MRF-OSHJ under MCE events.

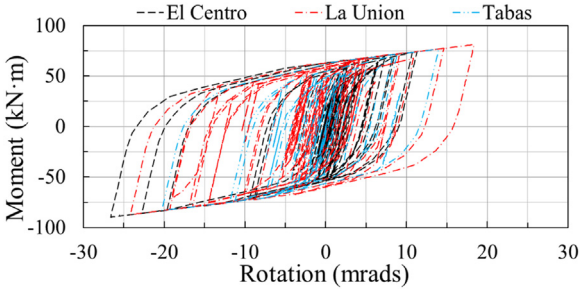

Fig. 11. Hysteretic responses of the first level OSHJ under MCE events.

Fig. 12 presents the maximum and average of maximum base shear, drift, and top storey acceleration responses of the structure to ULS and MCE events for the three earthquake records. On average, the ratio of the base shear response to MCE and ULS events is $^{200.9}/_{140.0} = 1.43$. Moreover, the MCE to ULS drift ratio is 2.04, and the acceleration ratio is 1.84. Based on a simplified multi degree of freedom model of the 13-storey Te Puni building, Ramhormozian et al. [30] reported that the kinematic hysteretic model could provide representative deflection envelop displacement but overestimate the residual drift. However, considering an elastic perfect plastic property was assigned in that model [30], the high return stiffness back to the loading line in quadrants 2 and 4 of the hysteresis curve were responsible for the higher-than-expected residual drift. For this study, with the inclusion of the post-elastic behaviour along the spine curve validated against the component test result for the OSHJ, shown in Fig. 7, a representative residual drift was generated by the model. Fig. 13 shows the residual inter-storey drift at three levels under both ULS and MCE events. The minimum residual inter-storey drift is overserved under El Centro event while the maximum residual inter-storey drift is overserved under Tabas event. The average maximum residual drift measured from the top storey is 0.11% and 0.29% under ULS and MCE, respectively. For a building to be satisfactory to avoid structural repair, the residual inter-storey drift limit was conservatively found to be ±0.14%, following the assessment of structures affected by the 2011 Christchurch earthquake [33]. The dynamic self-centring capability of the MRF-OSHJ is therefore satisfactory under the design level (ULS) earthquake.

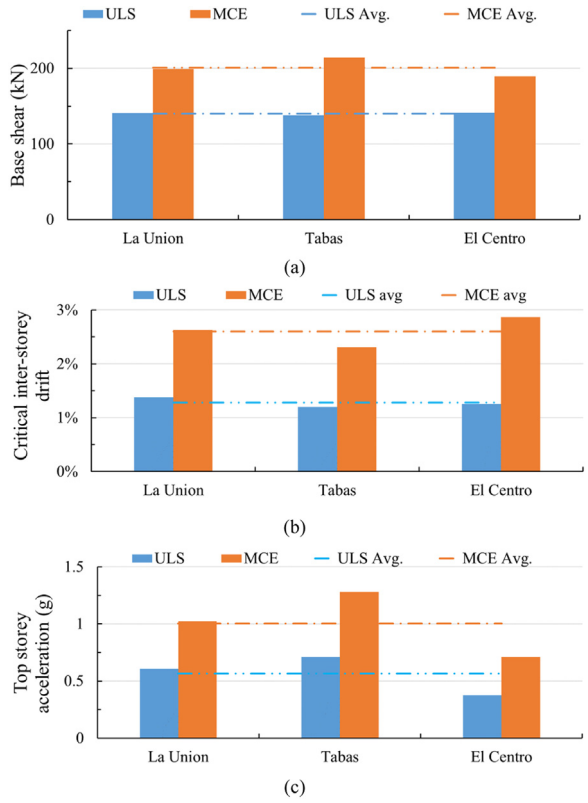

Fig. 12. Maximum and average of maximum (a) base shear, (b) critical inter-storey drift, and (c) top storey acceleration responses of the MRF-OSHJ to ULS and MCE events.

Fig. 14 shows the maximum and average demand of the connections at different stories to the ULS and MCE events. The rotation demands under ULS events are more evenly distributed than that under MCE events. On average, the ratio of the connections demand under MCE events to the connections demand under ULS events is 2.4.

To ensure reliable performance of the OSHJ and the overall structure during extreme earthquake events, the OSHJ is design to ensure that all bolts, that designed to slide, have sufficient slotted length to accommodate seismic drift under MCE. The length of the slotted hole is designed to accommodate $1.25 \times 3\% = 3.75\%$ rotation [15,21], where 1.25 is an over-rotation factor. The OSHJ is well within this rotation limit. It can also be seen that the La Union record (subduction interface) induces the largest OSHJ rotation amongst three records under ULS level shaking while El Centro record (strike-slip) induces the largest OSHJ rotation under MCE level shaking. To have a reliable estimation on joint rotation demand, both ULS and MCE events should be considered when conducting time-history analysis.

4. CBF-SFCBeSs configuration

As for the CBF-SFCBeSs concept, V-braced CBF is considered and designed in the transverse direction of the test structure. The SFCBeSses are then designed and detailed at brace to gusset plate connections (circled in red in Fig. 15), requiring minimum or no post-earthquake repair. Designed to slide before protected structural members yield, the SFCBeSs limit the internal axial actions of the brace to a pre-defined level. Similar to the MRF-OSHJ concept, the structure is designed to remain elastic under SLS, i.e., without sliding at the SFCBeSs. While the demand exceeds the design sliding shear force of the SFCBeSs under ULS, sliding commences, dissipating energy through friction. At the end of the earthquake events, the SFCBeSs seize up and become effectively rigid again. The focus of this section is to show the design procedures and develop a representative numerical model of the CBF-SFCBeSs to be tested on the shake table.

4.1. Member design using ESM

The design procedure for this configuration follows the requirement as per cl.12.12 NZS3404 [27] and HERA Report R4–76 [34] besides extra consideration on the C_s factor. The C_s factor presented in NZS 3404 [27] takes account of the less satisfactory inelastic behaviour of the CBF systems. It accounts for 1) the departure of the CBF system from the optimum O-mechanism system (plastic hinges spread throughout several levels of the structure [34]), 2) the less-than-ideal hysteretic behaviour of the CBF system and 3) the deterioration in inelastic performance. With the presence of the SFCBeSs at brace to gusset plate connection, the brace has a similar capacity in both compression and tension. The inelastic behaviour only occurs at the joint while the brace remains elastic during the sliding. Therefore, the C_s factor is taken as 1 regardless of the effect of the compression brace slenderness ratio. The fundamental period of the structure is estimated as per Eq. (2), where the factor, k_t, is taken as 0.05 and h_n is the height from the base of the structure to the uppermost seismic weight. The seismic forces applied to the lateral

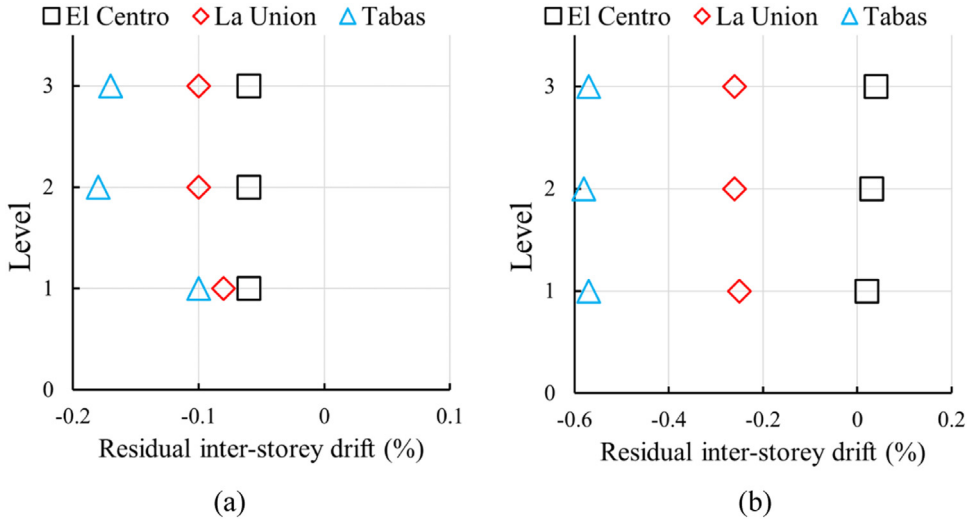

Fig. 13. Residual displacement at three levels under (a) ULS and (b) MCE events.

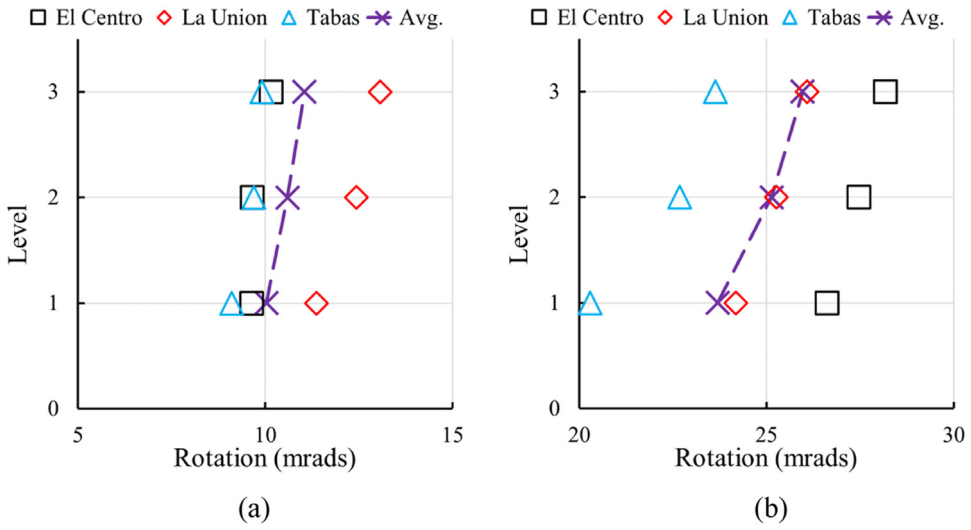

Fig. 14. Maximum and average of maximum rotation demands of the OSHJ to (a) ULS and (b) MCE events.

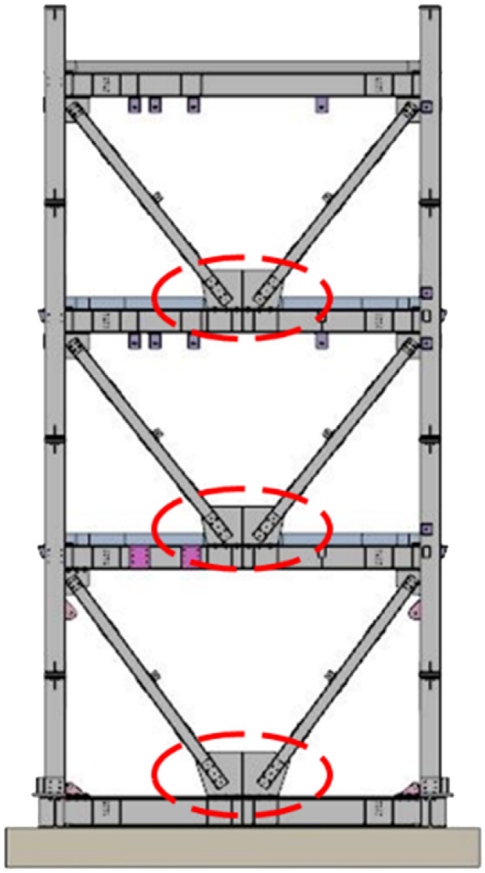

Fig. 15. Elevation view of the CBF-SFCBeSs concept.

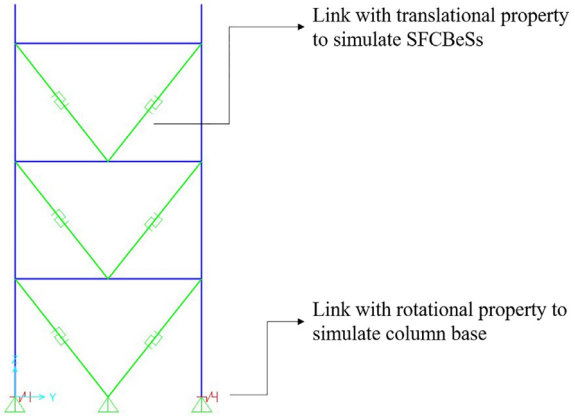

Fig. 16. Numerical model of the CBF-SFCBeSs in the transverse direction.

Table 7
Structures modal periods for the CBF-SFCBeSs concept.

Mode number	Mode period (s)
1	0.25
2	0.18
3	0.09

load resisting system can then be estimated using the ESM.

$$T_{1\_CBF} = 1.25 \times k_t \times h_n^{0.75} = 1.25 \times 0.05 \times 9^{0.75} = 0.325\text{s} \quad (2)$$

In the transverse direction, the braces can be modelled as linear elastic members, of which the sections assigned are based on the design action estimated from the ESM, i.e., design sliding shear force of the SFCBeSs. Alternatively, the SFCBeSs can be introduced and represented using elastic translational links (see Fig. 16), of which the elastic axial stiffness should be defined as Eq. (3).

$$k_{BeSFC} = \frac{EA}{L_{brace}} \quad (3)$$

where
E = Young's modulus
A = Cross sectional area of the incoming brace
L_{brace} = Length of the brace

The period of the structure should now be revised based on the modal analysis. The modal periods as well as SLS and ULS base shears are given in Tables 7 and 8 respectively. The first and third modes are translational and the second mode is torsional.

Following this initial design, nonlinear pushover and time-history analyses are carried out to study the performance and adequacy of the CBF-SFCBeSs concept more accurately. For this purpose, the non-linear behaviour of the SFCBeSs should be determined in SAP2000 using link element, defined for the axial translational degree of freedom. Plastic

Table 8
SLS and ULS base shears from ESM for the CBF-SFCBeSs concept.

Limit state	R	μ	S_p	Base shear (kN)
SLS	0.25	1	0.7	131.2
ULS	1.0	3	0.7	245.0
EQmax	1.0	1	0.7	459.3

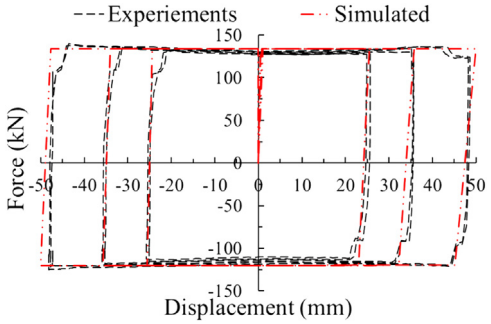

Fig. 17. Comparison of results for SFCBeSs brace-to-gusset plate subassembly.

(Wen) model [29] is used to generate the SFCBeSs hysteresis curve, based on the experimental results. The hysteretic model in comparison with experimental testing result is shown in Fig. 17 which shows good agreement.

4.2. Nonlinear static pushover analysis

Similar to the OSHJ, the SFCBeSses are designed such that no slippage occurs before the ULS base shear obtained from the ESM is reached, and also the maximum base shear on the pushover curve should be less than the upper limit base shear from the ESM. Determination of the SFCBeSs strength is initially based on the design actions obtained from the ESM directly. This means iterations may be required to finalize the required design capacity of the SFCBeSs to meet the design requirements for both SLS and ULS. The target ULS inter-storey drift is set to be less than 1.0%. Then the MCE level is taken as 1.8 times of the ULS drift. Hence, the target displacement at the top of the structure for ULS and MCE levels is to be less than 90 mm and 162 mm, respectively. However, there are a few special requirements of the ROBUST project which affects the selection of brace section, as follows:

1) different structural concepts are to be tested within one main frame (this means the design of primary members needs to satisfy all configurations); and
2) to adopt practical bolt size and layout for friction connections (i.e. the selection of brace section needs to meet the geometrical requirements from using appropriate HSFG bolts).

Table 9
Modal periods for the CBF-SFCBeSs concept.

Mode number	Mode period (s)
1	0.15
2	0.12
3	0.05

After consideration of back-to-back channels and RHS sections, the final solution adopted is back-to-back 160 × 80 × 6 RHS. The actual structure is considerably stiffer than the ideal design explained above. The updated modal periods are given in Table 9.

The first and third modes are translational, and the second mode is torsional. The quasi-static response of the structure up to 2.5% lateral drift (225 mm displacement at the top storey) is shown in Fig. 18, where the dashed horizontal lines indicate the SLS and ULS base shear.

The structure remains elastic before SLS base shear is reached and starts to become nonlinear when the ULS base shear is reached. To estimate the SFCBeSs displacement demand in the system at any level of drift, Eq. (4) can be used. As one of the purposes for using SFCBeSs is to have no structural damage in the system up to MCE, the SFCBeSses are designed to accommodate MCE displacement demand by providing sufficient slotted length. Therefore, the required sliding displacement of the SFCBeSs in one direction at the critical storey considering a drift level of 1.8 × 1%, to represent the MCE, is 32 mm.

$$\Delta_{\text{SFCBeSs}} = \sqrt{H^2 + \left(\frac{B}{2} + \Delta_{story}\right)^2} - L_{brace} \tag{4}$$

where
H = inter-storey height
B = span of the considered bay
Δ_{story} = storey drift

4.3. Nonlinear time history analysis

4.3.1. Scaling of earthquake records

The target and scaled spectrum to ULS for CBF-SFCBeSs is shown in Fig. 19.

4.3.2. Structure's dynamic responses incorporating CBF-SFCBeSs

The base shear response of the structure and the connection responses at each storey to MCE events are given in Fig. 20. The demand on the connections is less than the connection capacity. Thus, the design and detail of the connection is acceptable under selected earthquake records.

Fig. 21 presents the maximum and average of maximum base shear, drift, and top storey acceleration responses of the structure to ULS and MCE events. On average, the ratio of the base shear response to MCE and

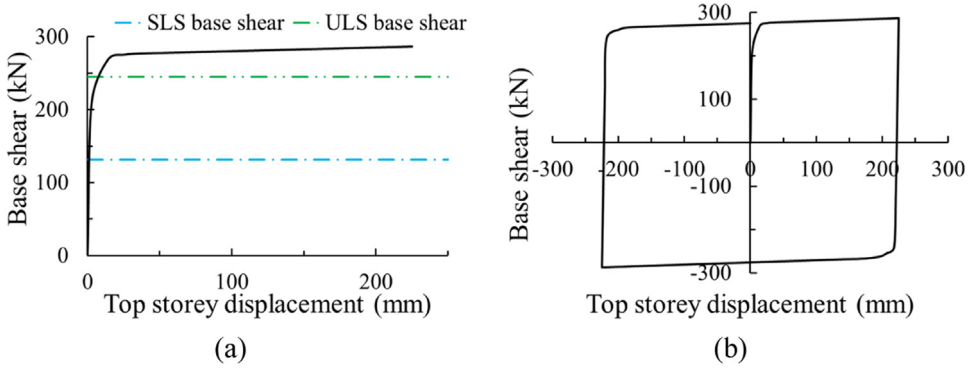

Fig. 18. V-braced CBF-SFCBeSs concept response to nonlinear static pushover analysis (a) uniaxial and (b) full cycle response.

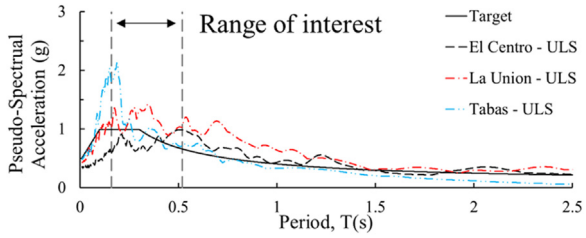

Fig. 19. Target and scaled records pseudo acceleration spectra.

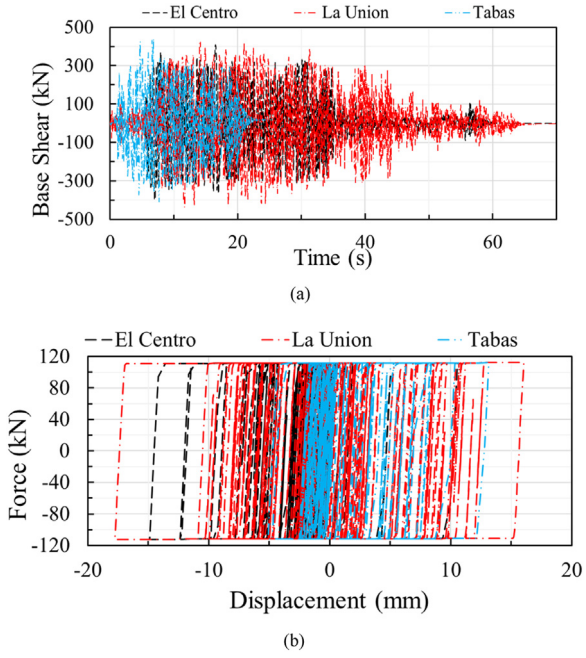

Fig. 20. (a) Base shear response and (b) SFCBeSs responses at first level to MCE events.

ULS events is $^{429}/_{344.4} = 1.25$. In addition, the average and maximum ULS base shears are higher than what obtained through ESM, which is 245 kN. The average and maximum MCE base shears are lower than the upper limit actions obtained from ESM, which is 459.3 kN. Moreover, the MCE to ULS drift and acceleration ratios are 3.57 and 1.5 respectively. The average maximum residual drifts measured from top storey under ULS (0.11%) and MCE (0.07%) are both below the 0.14% limit. It's also worth noting that in this case, the average maximum residual drift under the MCE is less than that under the ULS.

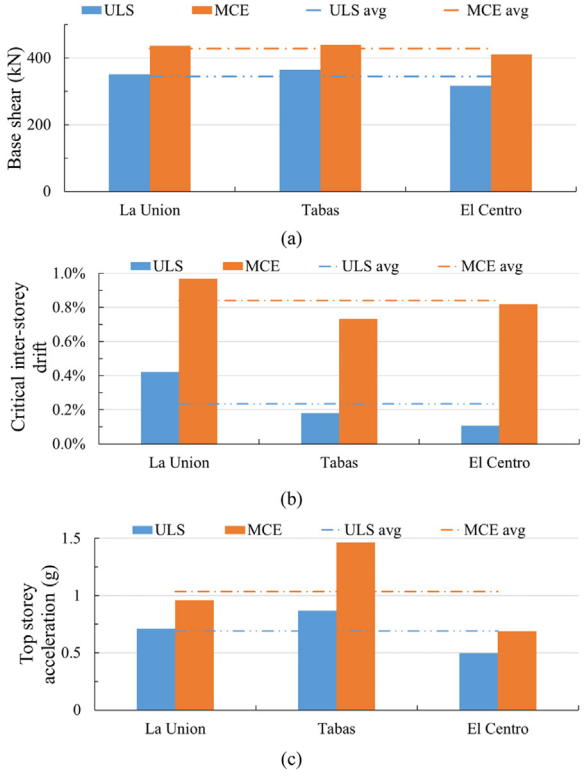

Fig. 21. Maximum and average of maximum (a) base shear, (b) drift, and (c) top storey acceleration responses of the CBF-SFCBeSs to ULS and MCE events.

Fig. 22 shows the maximum and average demand of the connections to ULS and MCE events at different stories. None of the joints reached their ultimate capacity (i.e., bolts in contact with the end of the slotted holes). The ratio of the average maximum sliding distance under MCE events to the average maximum sliding distance under ULS events is 3.7 for the CBF-SFCBeSs, which is 1.6 times higher than the ratio of the average maximum rotation under MCE events to the average maximum rotation under ULS events for the MRF-OSHJ.

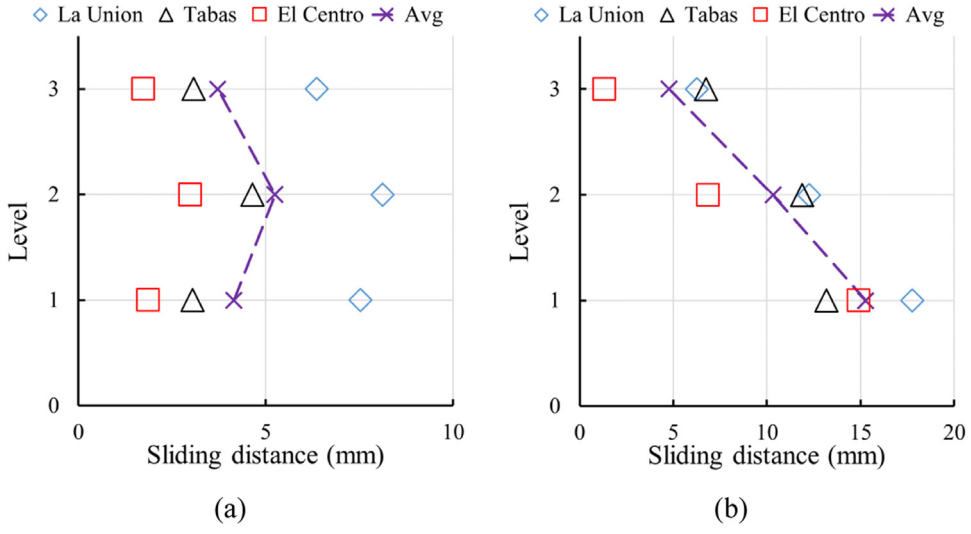

Fig. 22. Maximum and average of maximum sliding demands of the SFCBeSses to (a) ULS and (b) MCE events.

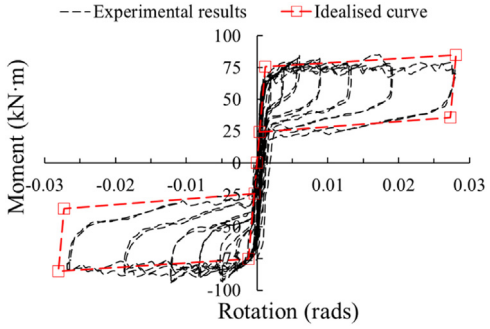

Fig. 23. Comparison of SAFC Base experimental results and idealized curve.

5. An alternative column base detail

The most common column base connection type for a MRSF is a fixed column base connection, which has the advantage of reducing lateral deflection in the superstructure [15]. The other option is to have a pinned column base, as presented in this study, which has the advantage of preventing hinge formation of column at its base. However, conventional column base connections might suffer from large plastic deformations and axial shortening phenomena, which can potentially suppress the building returning to the initial condition following severe earthquake events [35]. A friction-type column base connection i.e. column base strong axis-aligned asymmetric friction connection, noted as SAFC Base is a potential suitable column base detail for MRSF incorporating OSHJ concept. This is because it combines the benefits of the pinned base, in protecting the column from inelastic action at its base, with the ability to generate stable moment resistance with increasing rotation demand. A full-scale component test of SAFC Base tested at a constant axial load showed a flag shape hysteresis loop indicating good self-centring capacity (see Fig. 23), which may assist in returning the building to its pre-earthquake position.

6. Conclusions

This study presents the design, experimental component test results, and numerical studies of a low-damage three-storey steel framed structure. Hysteretic models for both OSHJ and SFCBeSs used in the numerical modelling and analysis, are developed based on real scale component tests. It is concluded that a structure with resilient performance is provided. Results are presented and analysed with the key conclusions outlined below:

- The MRF-OSHJ concepts showed satisfying performance under ULS and MCE earthquake records. None of the joints' inelastic demand exceeds the designed value. The distribution of the inelastic demand tends to be evenly distributed under ULS level earthquake. Even though assigned with nominal pinned column base, the contribution from rotational stiffness at column base is not negligible during pushover analysis. A more rigorous and realistic method for determining the initial rotational stiffness of the OSHJ is to be further investigated, as the current method may result in overestimating the stiffness or requiring iterations to an optimum design.
- The CBF-SFCBeSs concept shows a higher MCE to ULS ratio in terms of critical inter-storey drift and acceleration but significantly less in terms of base shear than that of the MRF-OSHJ. It is worth noting that a larger than required brace section is used to meet the required construability for SFCBeSs following suggested layout requiring two rows of bolt and two bolts per row without complicating the connection detail. Given the primary objective of the current research is 1) to investigate the seismic performance of the CBF-SFCBeSs concept while friction sliding connection's components, the brace, as well as beams and columns will remain elastic, and 2) to have a significantly stiffer system compared with the MRF-OSHJ, in the orthogonal direction to test different NSEs, the current design of the CBF-SFCBeSs is considered acceptable.
- The average maximum residual drift for the CBF-SFCBeSs is below ±0.14% under both ULS and MCE events. The average maximum residual drift for the MRF-OSHJ is below ±0.14% under ULS events, but slightly under MCE events. However, the influence of the composite floor slab and NSEs are not considered in the model though positive contributions are expected as described in [30]. Further coverage of this is outside the scope of this paper but will be addressed in ongoing research, including experimental testing without and then with the NSEs.
- The ratio of the connection deformation demand (rotation demand for the OSHJ and sliding demand for the SFCBeSs) under MCE events to the connection deformation demand under ULS events is 2.4 and 3.7 for the MRF-OSHJ and the CBF-SFCBeSs, respectively. This is greater than 1.8, especially for the CBF-SFCBeSs case. This ratio gives the designer an insight during the primary design of the structure for the MCE level, that there might be a need to verify the connection deformation demand.
- A solution for the column base connection is provided using SAFC Base, which combines the benefits of a pinned and fixed column base, preventing hinge mechanism and limiting inter-storey drift. The hysteretic model shows a flag shape response under a constant gravity load. More studies are to be undertaken to incorporate such characteristics considering varying gravity load, imposed on columns during earthquake events.

Declaration of Competing Interest

The authors declare that they have no known competing financial interests or personal relationships that could have appeared to influence the work reported in this paper.

Acknowledgements

This work described is part of a joint New Zealand (NZ) -China research programme with the International Laboratories on Earthquake Engineering (ILEE), Tongji University, Shanghai, China and directly with Tongji University, Shanghai, China. Direct NZ funding is kindly provided by the Building Research Association of NZ (BRANZ) under the Building Research Levy, the Earthquake Commission (EQC), the HERA Foundation (a charitable trust associated with HERA), QuakeCentre, the Tertiary Education Commission funded QuakeCoRE (the NZ ILEE partner through whom the NZ funding is also coordinated), and the University of Auckland (UA). Administrative support is provided by University of Canterbury (UC). Donations of materials is kindly provided by ComFlor, Hilti Corporation, Tracklok, Gripple, Lanyon & LeCompte Construction Ltd., and Alutech Doors & Windows Ltd. and Catalyst (GNG component tests). Expertise has been generously provided by a number of NZ industry representatives. The authors gratefully acknowledge this support. Opinions expressed are those of the authors alone. The QuakeCoRE paper number is 0811. The support from New Zealand Ministry of Business, Innovation and Employment (MBIE) through an Endeavour Fund for the Research Programme (Sustainable Earthquake Resilient Buildings for a Better Future - PROP-83779-ENDRP-AUT) is greatly appreciated.

References

[1] Clifton GC, MacRae GA. Lessons from the field; steel structure performance in earthquakes in New Zealand from 2010 to 2016. In: Key engineering materials, 763. Trans Tech Publications Ltd; 2018. p. 61–71.
[2] MacRae G, Clifton C, Innovations S. Low damage design of steel structures. Steel Innovations 2013 Workshop Christchurch, New Zealand; 2013.
[3] MacRae GA, Clifton GC. Research on seismic performance of steel structures. Proc of Steel Innovations 2015 Conference, 3 Auckland, New Zealand; 2015.

[4] MacRae GA, Clifton GC, Bruneau M. New Zealand research applications of, and developments in, low damage technology for steel structures. Key engineering materials 2018;763:3–10.
[5] Fang C, Wang W, Qiu C, Hu S, MacRae GA, Eatherton MR. Seismic resilient steel structures: a review of research, practice, challenges and opportunities. J Constr Steel Res 2022;191:107172.
[6] Yan Z, MacRae G, Dhakal R, Bagheri H, Clifton C, Quenneville P, Ramhormozian S, Zhao X, Jia L, Xiang P. Shaking table test of a near full scale low damage structural steel building: structural aspects. Paper presented at the Pacific Conference of Earthquake Engineering Auckland, New Zealand; 2019.
[7] Yan Z, Ramhormozian S, Clifton C, Bagheri H, MacRae G, Quenneville P, Zhao X, Jia LJ, Xiang P, Dhakal R. Shaking table testing of a three-storey steel frame building incorporating friction-based connections: structural design and detailing. Paper presented at the New Zealand Society for Earthquake Engineering Annual Technical Conference Wellington, New Zealand; 2020.
[8] Yan Z, Bagheri H, Ramhormozian S, Clifton C, Rangwani K, MacRae G, Quenneville P, Rodgers G, Xiang P, Jia LJ, Zhao X. Three-storey configurable steel framed building incorporating friction-based energy dissipaters: structural configuration and instrumentation. Paper presented at the New Zealand Society for Earthquake Engineering (NZSEE) Annual Technical Conference Christchurch, New Zealand; 2021.
[9] MacRae G, Zhao X, Jia L-J, Clifton GC, Dhakal R, Xiang P, Ramhormozian S, Rodgers G. The China-NZ ROBUST friction building shaking table testing overview. 17th World Conference on Earthquake Engineering, 17WCEE Sendai, Japan; 2020.
[10] Dhakal R, Rashid M, Bhatta J, Chen C, Song G, Sullivan TJ, MacRae G, Clifton GC, Jia L-J, Xiang P. Shake table testing plan for multiple non-structural elements & contents in a low-damage structural steel building. 17th World Conference on Earthquake Engineering, 17WCEE Sendai, Japan; 2020.
[11] Yan Z, Xie J, Rangwani K, Ramhormozian S, Xiang P, Jia L, Quenneville P, Dhakal R, Clifton C, MacRae G, Zhao X. Three-storey configurable steel framed building incorporating friction based energy dissipaters: overview of component test results. Poster presented at 2022 QuakeCoRE Annual Meeting Napier New Zealand; 2022.
[12] Wiebe LDA. Design and construction of controlled rocking steel braced frames in New Zealand. In: Improving the seismic performance of existing buildings and other structures 2015; 2015. p. 810–21.
[13] Cook J, Rodgers GW, MacRae GA. Design and testing of ratcheting, tension-only devices for seismic energy dissipation systems. J Earthquake Eng 2020;24(2):328–49.
[14] Xie R, Li Z, Xiang P, Jia LJ. Dynamic behaviours of steel multiple-rocking-column structural system with rocking stoppers. Eng Struct 2021;243:112649.
[15] Clifton GC. Semi-rigid joints for moment-resisting steel framed seismic-resisting systems (Doctoral dissertation, ResearchSpace@ Auckland). Department of civil and environmental engineering. Auckland, New Zealand: University of Auckland; 2005.
[16] Hashemi A, Zarnani P, Darani FM, Valadbeigi A, Clifton GC, Quenneville P. Damage avoidance self-centering steel moment resisting frames (MRFs) using innovative resilient slip friction joints (RSFJs). Key engineering materials 2018;763:726–34.
[17] Ramhormozian S, Clifton C, Gledhill S, Muller M. The optimised sliding hinge joint (OSHJ): design, detail, and implementation in practice; 2021.
[18] Bagheri H, Hashemi A, Yousef-Beik SMM, Zarnani P, Quenneville P. New self-centering tension-only brace using resilient slip-friction joint: experimental tests and numerical analysis. J Struct Eng 2020;146(10):04020219.
[19] NZS 1170.0:2002 — structural design actions part 0: general principles. Wellington, New Zealand: Standards New Zealand; 2002.
[20] NZS 1170.5:2004 — structural design actions earthquake actions. Wellington, New Zealand: Standards New Zealand; 2004.
[21] Ramhormozian S, Clifton C. HERA Report R4-155. Auckland, New Zealand: Heavy Engineering Research Association; 2021.
[22] Ramhormozian S, Clifton GC, MacRae GA, Davet GP. Stiffness-based approach for Belleville springs use in friction sliding structural connections. J Constr Steel Res 2017;138:340–56.
[23] Ramhormozian S, Clifton GC, MacRae GA, Davet GP, Khoo HH. Experimental studies on Belleville springs use in the sliding hinge joint connection. J Constr Steel Res 2019;159:81–94.
[24] Borzouie J, MacRae GA, Chase JG, Rodgers GW, Clifton GC. Experimental studies on cyclic performance of column base strong axis–aligned asymmetric friction connections. J Struct Eng 2016;142(1):04015078.
[25] Hyland C, Cowie K, Bird G. Structural steelwork connections guide: connection tables, SCNZ 14.2 2007. Manukau City: Steel Construction New Zealand (Inc); 2007.
[26] Hyland C, Cowie K, Clifton C. Structural steelwork connections guide: design procedures, SCNZ 14.1 2007. Manukau City: Steel Construction New Zealand (Inc); 2007.
[27] NZS 3404: steel structures standard. Wellington, New Zealand: Standards New Zealand; 1997.
[28] Clifton GC, Andisheh K, Hamid Z. HERA Report R4-156. Auckland, New Zealand: Heavy Engineering Research Association (HERA); 2022.
[29] CSi SAP2000, structural software for analysis and design; 2019.
[30] Ramhormozian S, Clifton GC, Latour M, MacRae GA. Proposed simplified approach for the seismic analysis of multi-storey moment resisting framed buildings incorporating friction sliders. Buildings 2019;9(5):130.
[31] Gledhill S, Sidwell G, Khoo HH, Clifton GC. Steel moment frames with sliding hinge joints—lessons learnt during implementation. In: Proceedings of the Steel Innovations Conference; 2013. p. 21–2.
[32] Oyarzo-Vera CA, McVerry GH, Ingham JM. Seismic zonation and default suite of ground-motion records for time-history analysis in the North Island of New Zealand. Earthquake Spectra 2012;28(2):667–88.
[33] Clifton GC. Lessons learned for steel seismic design from the 2010/2011 Canterbury Earthquake Series. In: Proceedings of the Australian Earthquake Engineering Society 2013 Conference; 2013. p. 15–17.
[34] Feeney MJ, Clifton GC. HERA Report R4-76. Auckland, New Zealand: Heavy Engineering Research Association; 2001.
[35] Elettore E, Freddi F, Latour M, Rizzano G. Parametric study and finite element analysis of self-centring steel column bases with different structural properties. J Constr Steel Res 2022;199:107628.